Comparison of Multistandard and TMS-Standard Calculated NMR Shifts for Coniferyl Alcohol and Application of the Multistandard Method to Lignin Dimers

ARTICLE *in* THE JOURNAL OF PHYSICAL CHEMISTRY B · FEBRUARY 2011

Impact Factor: 3.3 · DOI: 10.1021/jp110330q · Source: PubMed

3 AUTHORS:

Heath Watts
Pennsylvania State University
14 PUBLICATIONS **98** CITATIONS
SEE PROFILE

Mohamed Naseer ali Mohamed
The New College
15 PUBLICATIONS **149** CITATIONS
SEE PROFILE

J. D. Kubicki
University of Texas at El Paso
216 PUBLICATIONS **4,438** CITATIONS
SEE PROFILE

THE JOURNAL OF PHYSICAL CHEMISTRY B

ARTICLE

pubs.acs.org/JPCB

Comparison of Multistandard and TMS-Standard Calculated NMR Shifts for Coniferyl Alcohol and Application of the Multistandard Method to Lignin Dimers

Heath D. Watts,[†,‡] Mohamed Naseer Ali Mohamed,[†,‡] and James D. Kubicki*[,†,‡]

[†]Department of Geosciences and the Earth and Environmental Systems Institute and [‡]Center for NanoCellulosics, The Pennsylvania State University, University Park, Pennsylvania 16802, United States

ABSTRACT: Coniferyl alcohol is a monomeric building block of lignin, the second most abundant biopolymer. During lignification, the monomer forms a variety of linkages through free radical additions. A large NMR database has been constructed that reports the ^{1}H and ^{13}C chemical shifts for thousands of lignin oligomers. Herein, Boltzmann averaged ^{1}H and ^{13}C GIAO NMR calculations were performed on coniferyl alcohol and four of its dimers, β-O-4, β-β, β-5, and 5-5, to compare the calculated chemical shifts with experiment. Six B3LYP/6-311++G(d,p) energy-minimized conformational isomers of coniferyl alcohol were subjected to single-point GIAO NMR calculations. Initially, four NMR shift calculation methods were compared: three were performed using the TMS-standard method at the HF/6-311+G(2d,p), B3LYP/6-311+G(2d,p), and mPW1PW91/6-31G(d) theory levels, and the fourth was performed with a multistandard approach using a mPW1PW91/6-31G(d) theory level. For the multistandard method, benzene was used as the standard for aromatic C and H atoms and methanol was used for aliphatic C and H atoms. The hydroxyl-H of methanol was used as the standard for hydroxyl-H atoms. The Boltzmann averaged results for six conformers showed that the multistandard method is more accurate for coniferyl alcohol and its dimers than the often used TMS-standard method, based on the mean unsigned, root-mean-squared, and maximum errors, as well as linear correlations between observed and calculated values. The ^{13}C results were more accurate than the ^{1}H results, due to poorer agreement between calculated hydroxyl-H results and observed data. Further Boltzmann-averaged, multistandard NMR calculations compared the ^{13}C and ^{1}H chemical shifts with experiment for the four stereoisomers of the β-O-4 dimer, as well as the 5-5, β-5, and β-β dimers of coniferyl alcohol. The ^{13}C results correlated well with experiment ($r^2 > 0.99$) for all dimers and showed small statistical errors, compared with experiment. The correlation with experiment for ^{1}H NMR was generally inferior to the ^{13}C NMR results for the dimers.

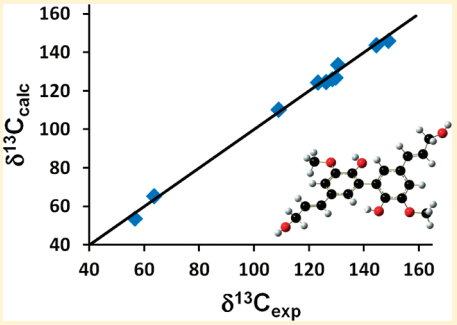

INTRODUCTION

Coniferyl alcohol (Figure 1, MG) is one monomeric building block of the hydrophobic biopolymer lignin, which is the second most abundant biomolecule; lignin forms by the combinatorial addition of the phenoxide radicals of 4-hydroxyphenyl-propanoids, like coniferyl alcohol.[1−3] The five most commonly studied linkages that form between two phenoxide radicals of coniferyl alcohol [IUPAC: 4-(3-hydroxy-1-propenyl)-2-methoxyphenol or commonly 4-hydroxy-3-methoxycinnamyl alcohol] include the β-O-4, β-β, β-5, and 5-5 linkages (Figure 1). These linkages correspond to 1-(4-hydroxy-3-methoxyphenyl)-2-[4-(3-hydroxypropenyl)-2-methoxyphenoxy]propane-1,3-diol (guaiacylglycerol-β-coniferyl ether), pinoresinol, 4-[3-hydroxymethyl-5-(3-hydroxypropenyl)-7-methoxy-2,3-dihydrobenzofuran-2-yl]-2-methoxyphenol, and 5,5-dehydrodiconiferyl alcohol, respectively.[2,4] Hereafter, the linkages will be referred to as the β-O-4, β-β, β-5, and 5-5 linkage, and coniferyl alcohol will be referred to as MG, denoting the primary monomer form of guaiacyl alcohol.[5]

Understanding the form and function of lignin will provide information necessary to better understand the biochemistry of cell walls and may also provide valuable information pertinent to lignin degradation for plant-based biofuel production.[6] Lignin forms through combinatorial, nonbiologically mediated free radical addition reactions,[2] while some evidence suggests that lignin may form through the action of dirigent proteins.[7−9] Evidence supports the combinatorial mechanism, which results in each lignin being a unique biopolymer, thus making the characterization of universal lignin polymer unlikely. Fortunately, studying the constituent dimers and oligomers of lignin with experimental[2,3,5] and computational chemistry[10−12] can provide valuable information about the short- and medium-sized structures of this important biopolymer. Prior computational chemistry studies of coniferyl alcohol and its dimers have focused on the energetics,[10−15] structure and reactivity,[16−18] and spectroscopic properties including Raman, UV−vis, infrared, and NMR.[19−22]

A large database of experimental NMR spectra for the constituent monomers, dimers, trimers, and tetramers of lignin is

Received: October 28, 2010
Revised: January 18, 2011
Published: February 14, 2011

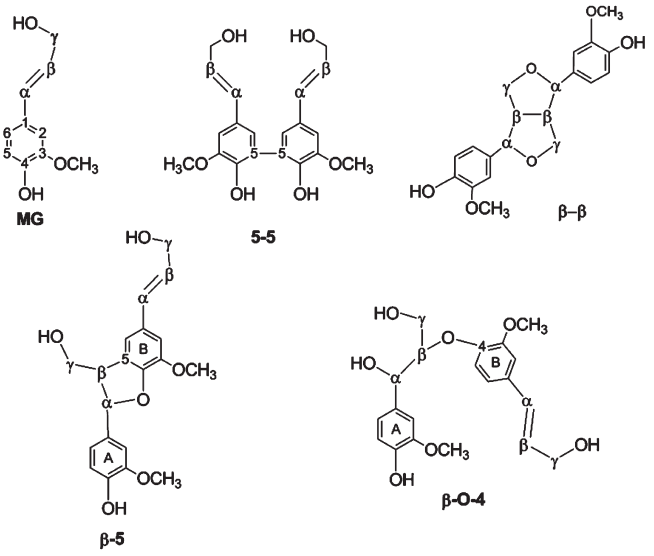

Figure 1. Coniferyl alcohol (MG) and its linkages used for this study. Aromatic rings that are not redundant due to symmetry are labeled as A or B for the MG dimers.

available;[4] however, to our knowledge, there has been no prior work comparing calculated NMR results with data for the β-O-4, β-5, β-β, and 5-5 lignin linkages, although two studies reported calculated NMR shifts for coniferyl alcohol (MG).[20,22] The results from one computational NMR study for MG found good correlation with experiment ($r^2 = 0.991$), but the mean unsigned error (4.9 ppm), root-mean-squared error (5.7 ppm), y-intercept (−11.8 ppm), and maximum error (10.8 ppm) associated with their methodology were relatively large.[22]

This work will improve the accuracy of calculated ^{13}C NMR shifts for coniferyl alcohol, relative to experiment, by incorporating a multistandard approach to NMR calculations and comparing those results to the tetramethylsilane (TMS) NMR reference standard approach.[23−25] The advantage of the multistandard method is that results of experimental quality can be obtained using a less computationally expensive basis set.[25] Additionally, this work will compare the ^{1}H NMR shifts for coniferyl alcohol, calculated with both the TMS standard and multistandard methods with experiment;[23−25] there have been no previous computational studies reporting ^{1}H NMR shifts for MG. More notably, this work will be the first to compare ^{1}H and ^{13}C NMR shifts for the β-O-4, β-β, β-5, and 5-5 linked MG dimers (Figure 1), calculated using the multistandard method, with experimental NMR database chemical shifts.[4] Additionally, this work uses Boltzmann averaged energies from six conformers of MG to attain a more accurate correlation between calculated and experimental NMR shifts for coniferyl alcohol and the dimers of interest.[26]

A major goal of this work is to determine a reliably accurate method for calculating ^{13}C and ^{1}H NMR shifts for lignin oligomers. Once verified, this method can then be tested and applied to larger polymers of lignin, and thereafter could be useful for NMR elucidation of polymer interactions in plant cell walls, such as lignin−hemicellulose interactions.[27]

METHODS

All models were built using Cerius^2 (version 4.9, Accelrys Inc.) and were energy minimized in the gas phase without symmetry or atomic constraints using Gaussian 03.[28] Subsequent frequency calculations ensured that a potential energy surface (PES) local minimum was attained during the energy minimization.[29,30] Energy minimizations and frequency calculations were performed using density functional theory (DFT)[31,32] with the hybrid density functional B3LYP[33−35] coupled with the 6-311++G(d,p) Pople-type basis set.[36,37] All single-point NMR GIAO calculations[38−41] were executed using the self-consistent reaction field (SCRF) method, applying the integral equation formalism variant of the polarized continuum model (IEFPCM) using the permittivity constants for acetone, dimethylsulfoxide (DMSO), and chloroform ($CHCl_3$) for C, while only acetone was used for H to more closely approximate experimental solvent conditions.[4,42,43] The GIAO NMR results were observed and extracted using GaussView 03.[28]

The β-O-4 model (Figure 1) has two chiral centers at its respective α and β C atoms; therefore, each dimer has four possible stereoisomers: RR or SS for the *threo* form, and RS or SR for the *erythro* form.[11] NMR data have been reported for the *threo* or *erythro* chemical shifts for the β-O-4 linkage;[4] therefore, this work evaluated the chemical shifts of the four stereoisomers of the β-O-4 linkage. Because the *threo* and *erythro* stereoisomers are racemic, the RR and SS stereoisomer results were compared with the experimental *threo* data, and the RS and SR stereoisomers with the *erythro* data. Hereafter, the RR, SS, RS, and SR nomenclature will be used in reference to the stereoisomers of the models.[11]

Figure 1 shows the number-labeling scheme used for the C atoms of the MG model and for the atoms pertinent to the dimer linkages used in this study. The aromatic rings of the β-5 and β-O-4 dimer linkages are labeled as either A or B; however, because these labels are redundant by symmetry for the 5-5 and β-β linkages, no distinction will be applied to the aromatic rings of those two structures. For the β-5 and β-O-4 linkages, all NMR shift results for the ^{1}H or ^{13}C nuclei will refer to the ring containing each particular nucleus. For example, the γ-H atoms of the β-5 structure will be discussed as either AHγ or BHγ, depending upon which ring, A or B, these H atoms are associated with (Figure 1). Conversely, the γ-H atoms on the 5-5 linkage are equivalent, so no label is necessary to distinguish between the nuclei associated with the aromatic rings of this structure (Figure 1).

Eight different conformers of MG were built using Cerius^2 because initial calculations showed poor agreement with experiment for aromatic C2; this discrepancy was corrected by using MG models with various C2−C3−O3−C_{OMe} (ω_1), C3−C4−O4−H4 (ω_2), and C2−C1−Cα−Hα (ω_3) dihedral angles (Figure 2).[44,45] Two of the eight initial structures energy optimized to redundant structures with energies, NMR shifts, and frequencies that were identical to two other structures, respectively; therefore, only six of the initial eight structures will be considered (Figure 2).

Each gas-phase, energy minimized structure of the six coniferyl alcohol conformers was then subjected to single-point GIAO[38−41] NMR calculations in a polarized continuum[42,43] of either acetone, chloroform, or DMSO using either the Hartree−Fock (HF) or B3LYP methods,[33−35,46] combined with the 6-311+G(2d,p) basis set.[24,36,37] Additional single-point GIAO NMR calculations, using the mPW1PW91[47] hybrid density functional coupled with the 6-31G(d) basis set, in a polarized continuum of acetone, chloroform, or DMSO, were performed for each of the six MG models to determine the effect of using multiple standards for calculating NMR shifts for coniferyl alcohol, compared with those obtained from the single standard (TMS) reference method.[24,25]

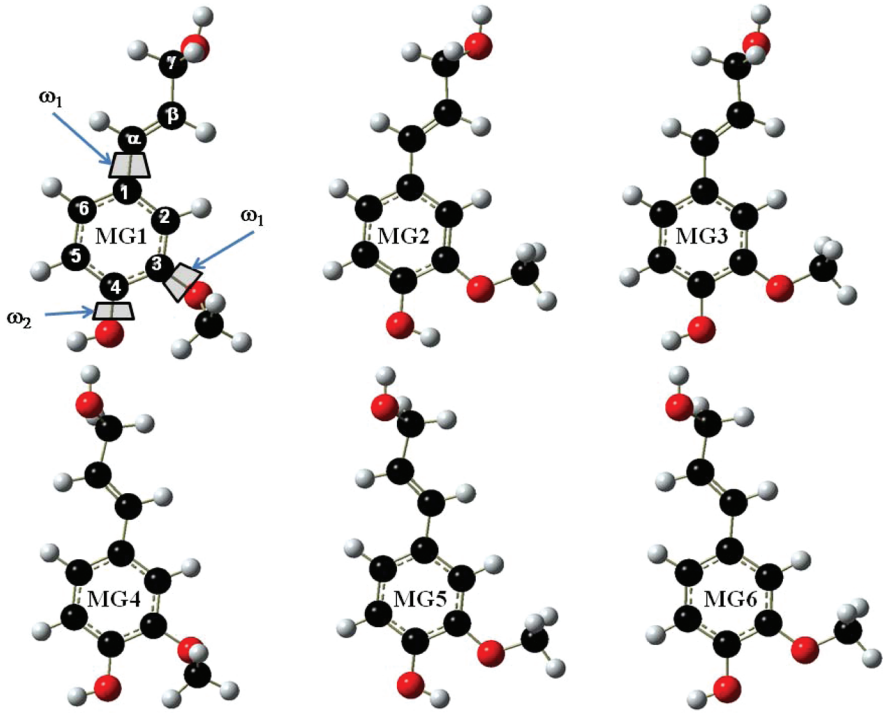

Figure 2. Energy minimized coniferyl alcohol conformers. The dihedral angles varied in this study [C2−C3−O3−C_{OMe} (ω_1), C3−C4−O4−H4 (ω_2), and C2−C1−Cα−Hα (ω_3)] are labeled for structure MG1 and marked with trapezoidal planes, which are perpendicular to the C1−Cα, C3−O3, and C3−O3 bonds, respectively.

Table 1. Boltzmann-Averaged Solvation Gibbs Free Energies for the Six Conformers of MG[a]

SCRF=IEFPCM method	standard method	MG conformer	$\langle N \rangle/N$ acetone	$\langle N \rangle/N$ $CHCl_3$	$\langle N \rangle/N$ DMSO
mPW1PW91/6-31G(d)	multistandard and TMS-standard	MG1	0.01	0.00	0.01
mPW1PW91/6-31G(d)	multistandard and TMS-standard	MG2	0.35	0.48	0.30
mPW1PW91/6-31G(d)	multistandard and TMS-standard	MG3	0.08	0.02	0.10
mPW1PW91/6-31G(d)	multistandard and TMS-standard	MG4	0.01	0.00	0.01
mPW1PW91/6-31G(d)	multistandard and TMS-standard	MG5	0.46	0.49	0.44
mPW1PW91/6-31G(d)	multistandard and TMS-standard	MG6	0.09	0.02	0.14
B3LYP/6-311+G(2d,p)	TMS-standard	MG1	0.01	0.00	0.02
B3LYP/6-311+G(2d,p)	TMS-standard	MG2	0.29	0.47	0.23
B3LYP/6-311+G(2d,p)	TMS-standard	MG3	0.13	0.03	0.15
B3LYP/6-311+G(2d,p)	TMS-standard	MG4	0.01	0.00	0.02
B3LYP/6-311+G(2d,p)	TMS-standard	MG5	0.40	0.47	0.35
B3LYP/6-311+G(2d,p)	TMS-standard	MG6	0.16	0.03	0.23
HF/6-311+G(2d,p)	TMS-standard	MG1	0.15	0.04	0.19
HF/6-311+G(2d,p)	TMS-standard	MG2	0.17	0.42	0.12
HF/6-311+G(2d,p)	TMS-standard	MG3	0.13	0.03	0.14
HF/6-311+G(2d,p)	TMS-standard	MG4	0.11	0.04	0.13
HF/6-311+G(2d,p)	TMS-standard	MG5	0.27	0.44	0.20
HF/6-311+G(2d,p)	TMS-standard	MG6	0.17	0.03	0.22

[a] $\langle N \rangle/N$ represents the Boltzmann weighting factor that each conformer contributes to the total energy. In all cases, MG2 and MG5 are the most thermodynamically stable conformers of those studied.

The six conformers studied herein form a small subset of all possible conformers that could be present experimentally, and each of these conformers will contribute to the observed chemical shifts, based on their thermodynamic stability. Moreover, a conformer that provides well-correlated NMR results may not be the most energetically favorable. A compromise between chemical accuracy and computational cost is necessary; for this work, six conformers provided good results, but additional conformers could further improve the results. Therefore, to estimate the contribution of each conformer to the calculated NMR chemical shifts, the ^1H or ^{13}C chemical shift of each H or C atom, for a given conformer, was expressed as the Boltzmann-weighted

Table 2. Boltzmann-Averaged ^{13}C and ^{1}H NMR Shifts in Acetone for Coniferyl Alcohol Using B3LYP/6-311++G(d,p) Energy Minimized Structures To Compare the Multistandard, mPW1PW91/6-31G(d) Method with the TMS-Standard B3LYP/6-311+G(2d,p), HF/6-311+G(2d,p), and mPW1PW91/6-31G(d) Methods[a]

			multistandard ^{13}C values	TMS-standard ^{13}C values					multistandard ^{1}H values	TMS-standard ^{1}H values		
statistic	^{13}C	exptl (ppm)	mPW1PW91 (ppm)	B3LYP (ppm)	HF (ppm)	mPW1PW91 (ppm)	^{1}H	exptl (ppm)	mPW1PW91 (ppm)	B3LYP (ppm)	HF (ppm)	mPW1PW91 (ppm)
	1	130.2	128.0	136.1	134.9	123.5	2	7.0	6.4	7.2	7.6	6.7
	2	109.9	111.1	113.7	119.9	106.7	OMe	3.9	3.9	4.0	3.8	3.8
	3	147.1	145.2	154.4	151.6	140.6	4OH	7.6	8.6	5.8	5.8	5.4
	4	148.4	145.3	154.5	153.7	140.6	5	6.8	6.6	7.3	7.5	7.0
	5	115.7	115.0	119.1	121.0	110.6	6	6.8	6.9	7.5	7.8	7.2
	6	120.6	121.0	124.8	128.2	116.6	α	6.5	6.1	6.9	7.0	6.5
	α	130.4	133.4	139.4	137.2	128.9	*β*	6.2	6.2	6.7	6.8	6.5
	β	128.0	125.9	131.6	132.4	121.5	*γ*	4.2	4.4	4.6	4.2	4.4
	γ	63.4	65.2	70.6	61.5	66.4	*γ*-OH	3.8	4.4	1.7	2.1	1.3
	OMe	56.1	53.4	56.7	53.2	54.6						
slope			0.99	1.04	1.09	0.92			0.94	1.10	1.17	1.07
y-intercept (ppm)			0.87	1.07	−6.10	5.69			0.44	−0.69	−1.01	−0.82
r^2			0.996	0.996	0.993	0.996			0.901	0.713	0.756	0.679
MUE (ppm)			1.9	5.1	5.3	2.5			0.3	0.7	0.8	0.7
RMSE (ppm)			2.1	5.6	5.8	3.4			0.5	1.0	1.0	1.1
ME (ppm)			3.2	9.0	10.0	5.7			0.9	2.0	1.8	2.5

[a] All calculations were performed using six conformers of coniferyl alcohol, MG1—MG6 (Figure 2).

average of the ^{1}H or ^{13}C chemical shift result.[26] The calculated solvation Gibbs free energy for each conformer was used to determine the Boltzmann weighting factors, because the experimental data was provided in acetone, $CHCl_3$, and DMSO; performing the Gibbs free energy and NMR tensor calculations in a continuum solvent was done to provide a better approximation of experimental techniques. The Gibbs free energy of solvation ($\Delta G°_{solv}$) was calculated by summing the total free energy in solution with all nonelectrostatic terms from the polarized continuum calculation plus the thermal correction to Gibbs free energy form the gas-phase frequency calculation. The Boltzmann-averaged chemical shifts were calculated using the methodology of Barone et al.[26]

To obtain the calculated chemical shifts of the nuclei from the respective MG calculation using the TMS-standard method,[24] the continuum solvated shielding tensors for each ^{1}H and ^{13}C atom in the a given conformer was subtracted from the HF/6311+G(2d,p)//B3LYP/6-311++G(d,p), B3LYP/6-311+G(2d,p)//B3LYP/6-311++G(d,p), or mPW1PW91/6-31G(d)//B3LYP/6-311++G(d,p) calculated TMS ^{1}H and ^{13}C shielding tensors, respectively. The $\Delta G°_{solv}$ Boltzmann-weighted factors for each conformer were then used to find the Boltzmann-averaged chemical shifts for each nucleus of the six conformers. The Boltzmann-averaged chemical shifts were then compared with the experimental chemical shifts, using the results and data for the relevant solvents.

For the multistandard method, the mPW1PW91/6-31G(d)//B3LYP/6-311++G(d,p) calculated shielding tensors were compared with the shielding tensors from either benzene, for sp^2 hybridized C atoms, or methanol, for sp^3 hybridized C atoms.[25] The NMR tensors for benzene and methanol were calculated using the mPW1PW91/6-31G(d)//B3LYP/6-311++G(d,p) method. The calculated chemical shift for a given C was calculated using the following equation:[25]

$$\delta^{x}_{calc} = \sigma_{ref} - \sigma_x + \delta_{exp}$$

Here σ_{ref} is the calculated shielding tensor of C from either benzene or methanol, σ_x is the shielding tensor for a C in the model of interest, and $\delta_{exp,ref}$ is the experimental chemical shift of C from either benzene (128.37 ppm) or methanol (50.41 ppm), relative to TMS.[25] The Boltzmann-averaged chemical shift results were then compared with the data.

Additionally, the results from the multistandard approach for the six conformers of MG were used to compare with the TMS method results, relative to the experimental NMR data for ^{1}H nuclei; application of the multistandard approach to H nuclei, to our knowledge, has not been previously reported for MG or its linkages. The reference compounds were once again benzene or methanol, which were used to calculate the chemical shifts of the aromatic or aliphatic/hydroxyl-H atoms, respectively. The same equation was used for these calculations, but here the $\delta_{exp,ref}$ values for benzene aromatic and methanol aliphatic H atoms are 7.34 and 3.43 ppm, respectively; the $\delta_{exp,ref}$ for hydroxyl-H atoms is 3.66 ppm.[48] The Boltzmann-averaged ^{1}H NMR results were then compared with the data.

Boltzmann-averaged, multistandard, solvated, single-point GIAO ^{1}H and ^{13}C NMR chemical shifts using the mPW1PW91/6-31G(d)// B3LYP/6-311++G(d,p) method for the *β*-O-4, *β*-*β*, *β*-5, and 5-5 MG dimers (Figure 1) were also compared with experimental data.

The Boltzmann-averaged chemical shift for each ^{13}C and ^{1}H in each model was calculated and compared with the chemical shift of the respective nuclei from experiment.[24] To statistically compare the calculated results with the experimental data, the

dx.doi.org/10.1021/jp110330q |J. Phys. Chem. B 2011, 115, 1958–1970

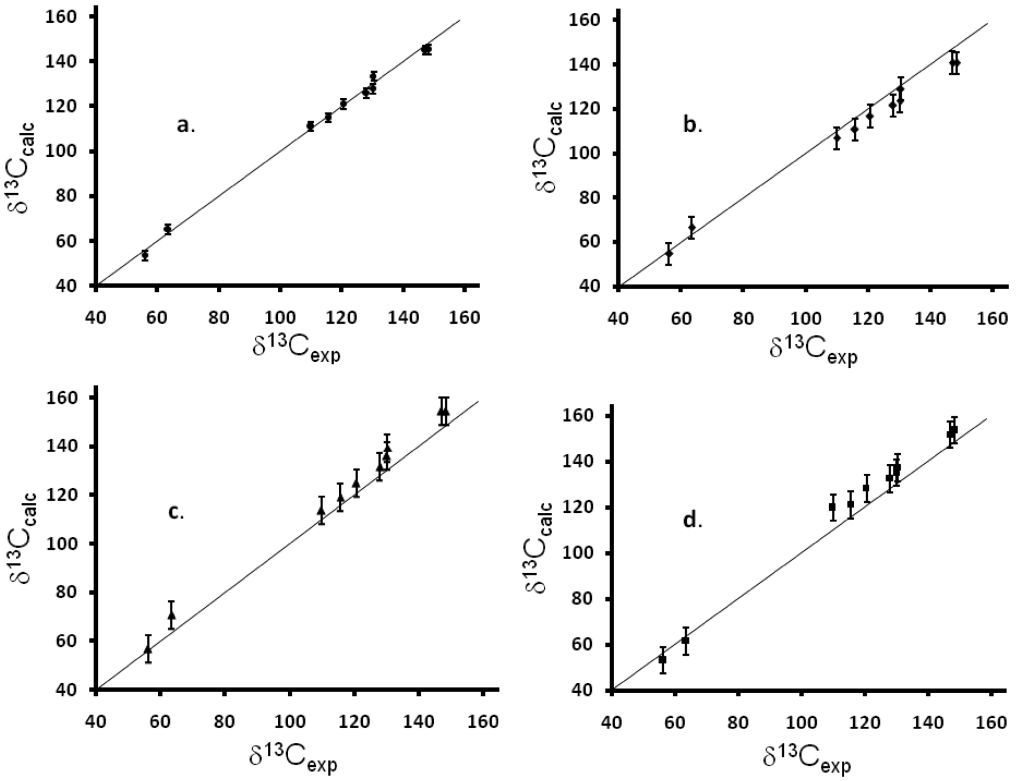

Figure 3. δ ^{13}C NMR calculation method comparison; all energy minimized with B3LYP/6-311++G(d,p). The NMR results are the Boltzmann averaged shifts for six coniferyl alcohol conformers (Figure 2). The panels show the results for (a) the mPW1PW91/6-31G(d) multistandard method, and the TMS-method results for (b) mPW1PW91/6-31G(d), (c) B3LYP/6-311+G(2d,p), and (d) HF/6-311+G(2d,p). All chemical shifts are in ppm, and the straight lines are the 1:1 lines, where δ $^{13}C_{calc}$ = δ $^{13}C_{exp}$. The error bars show the RMSE of 2.1, 5.0, 5.6, and 5.8 ppm for plots a−d, respectively.

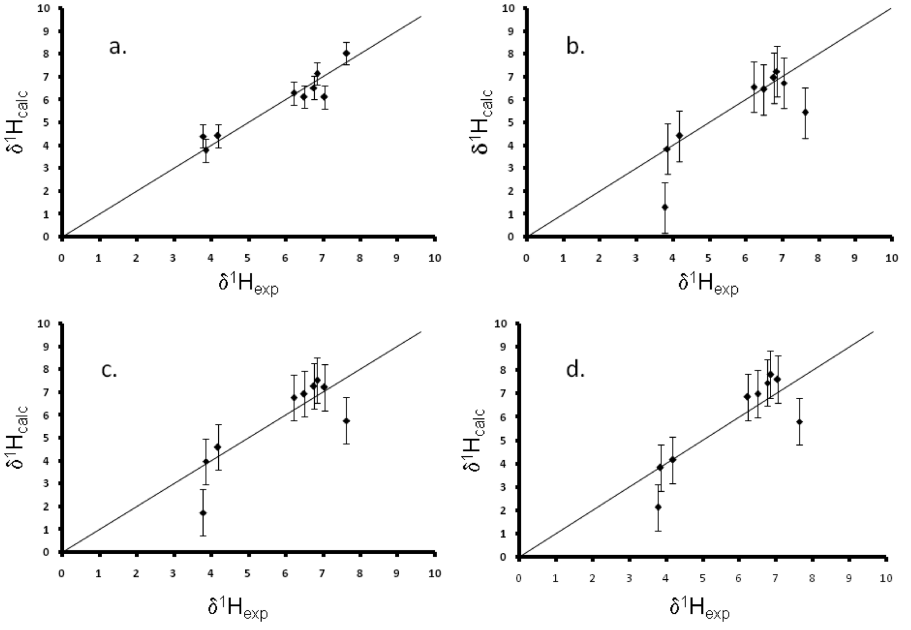

Figure 4. δ ^{1}H NMR calculation method comparison, all energy minimized with B3LYP/6-311++G(d,p). The NMR results are the Boltzmann averaged shifts for the six coniferyl alcohol conformers (Figure 2). The panels show the results for (a) the mPW1PW91/6-31G(d) multistandard method, and the TMS-method results for (b) mPW1PW91/6-31G(d), (c) B3LYP/6-311+G(2d,p), and (d) the HF/6-311+G(2d,p). All chemical shifts are in ppm, and the straight lines are the 1:1 lines, where δ $^{1}H_{calc}$ = δ $^{1}H_{exp}$. The error bars show the RMSE of 0.5, 1.1, 1.0, and 1.0 ppm for plots a−d, respectively.

slope, intercept, and correlation coefficient for each comparison were calculated using the Boltzmann-averaged results relative to the data.[22] Additionally, the mean unsigned (absolute) error (MUE) and the root-mean squared error (RMSE) were

Table 3. Linear Regression Coefficients and Error Statistics for the Boltzmann-Averaged NMR Shift Results for Six Coniferyl Alcohol Conformers (Figure 2) Compared with Experimental Data in $CHCl_3$ or DMSO[a]

	$CHCl_3$				DMSO			
statistic	$mPW1PW91_{MS}$	$B3LYP_{TMS}$	HF_{TMS}	$mPW1PW91_{TMS}$	$mPW1PW91_{MS}$	$B3LYP_{TMS}$	HF_{TMS}	$mPW1PW91_{TMS}$
slope	1.00	1.05	1.11	0.93	0.99	1.03	1.09	0.92
y-intercept (ppm)	−0.12	−0.02	−7.91	3.77	2.00	2.31	−4.66	5.65
r^2	0.997	0.997	0.996	0.997	0.995	0.994	0.993	0.994
MUE (ppm)	1.4	5.7	5.7	1.9	1.9	6.1	5.9	4.3
RMSE (ppm)	1.6	6.2	6.0	2.3	2.2	6.6	6.7	4.7
ME (ppm)	2.5	9.0	8.1	3.8	4.4	10.4	11.3	7.4

[a] The subscripts MS and TMS refer to the multistandard and TMS-standard NMR calculation methods, respectively.

Table 4. Boltzmann-Averaged Solvation Gibbs Free Energies for the MG Linkages[a]

MG linkage	MG conformer	$\langle N\rangle/N$ acetone	$\langle N\rangle/N$ $CHCl_3$	$\langle N\rangle/N$ DMSO
5-5	MG1	0.00		
5-5	MG2	0.34		
5-5	MG3	0.00		
5-5	MG2/MG3	0.12		
5-5	MG4	0.00		
5-5	MG5	0.53		
5-5	MG6	0.00		
threo (R,R)-*β*-O-4	MG2	0.00	0.00	0.00
threo (R,R)-*β*-O-4	MG5	0.00	0.00	0.00
threo (S,S)-*β*-O-4	MG2	0.38	0.50	0.36
threo (S,S)-*β*-O-4	MG5	0.62	0.49	0.63
erythro (R,R)-*β*-O-4	MG2	0.01	0.02	0.01
erythro (R,R)-*β*-O-4	MG5	0.04	0.07	0.07
erythro (S,S)-*β*-O-4	MG2	0.21	0.23	0.19
erythro (S,S)-*β*-O-4	MG5	0.74	0.68	0.73
β-5	MG2	0.50	0.54	0.47
β-5	MG5	0.50	0.46	0.53
β-*β*		NA	NA	NA

[a] The 5-5 linkage was evaluated with seven conformers. Thereafter, only the MG2 and MG5 forms were considered because they were the most energetically stable conformers based on the Boltzmann-averaged energies for the 5-5 dimer and MG monomer results (Table 1). The *β*-*β* conformer structure is identical for the MG2 and MG5 forms. $\langle N\rangle/N$ represents the Boltzmann weighting factor that each conformer contributes to the total energy.

calculated and reported in parts-per-million (ppm) for each model to statistically compare the Boltzmann-averaged results with the data.[24,25,49] The MUE was calculated using the formula

$$\mathrm{MUE} = \sum |\delta_x\text{-}\delta_{\mathrm{exp},x}|/N$$

where δ_x and $\delta_{\mathrm{exp},x}$ and are the Boltzmann averaged calculated and experimental chemical shifts of nuclei x, respectively, and N is the number of either the ^1H or ^{13}C nuclei in the compound.[49] The RMSE is calculated using

$$\mathrm{RMSE} = \sqrt{\left(\sum \left(|\delta_x\text{-}\delta_{\mathrm{exp},x}|\right)^2/N\right)}$$

The unsigned maximum error (ME) for each comparison is reported in ppm.

RESULTS AND DISCUSSION

TMS Standard versus Multistandard Method for Coniferyl Alcohol. Table 1 shows the Boltzmann weighting factors for the six conformers of coniferyl alcohol (Figure 2) in acetone, $CHCl_3$, and DMSO. The numbers indicate the fractional prevalence of each conformer, based on its weighted $\Delta G°_{solv}$; for example, the fractional prevalence of the conformer MG2 in acetone, $CHCl_3$, and DMSO using the mPW1PW91/6-31G(d) method is 0.35, 0.48, and 0.30, respectively. The sum of each set of weighting factors sums to one; for example for acetone, using the mPW1PW91/6-31G(d) method, the sum of the weighting factors for MG1 through MG6 is 1. Table 2 shows the experimental and calculated Boltzmann-averaged chemical shifts for MG in acetone for the ^{13}C and ^1H; Figures 3 and 4 graphically represent the results in Table 1, with the error bars showing the RMSE in ppm. Note that all lines, on all graphs, in all figures are the 1:1 lines, where $\delta_{calc} = \delta_{exp}$. The MG results indicate that the MG2 and MG5 conformers are energetically favored, regardless of solvent or method (Table 1).

While the ^{13}C results for the TMS-standard and multistandard methods provide nearly 1:1 correlations with the data (Table 2 and Figure 3), the error statistics indicate that the multistandard method out-performs the TMS-standard methods. The MUE, RMSE, and ME for the multistandard, mPW1PW91/6-31G(d) method (1.9, 2.1, and 3.2 ppm, respectively) are approximately

Table 5. Boltzmann-Averaged ^{13}C and ^{1}H NMR Shifts in Acetone for the 5-5 Coniferyl Alcohol Linkage Using the Multistandard, mPW1PW91/6-31G(d)//B3LYP/6-311++G(d,p) Method[a]

	^{13}C shift			^{1}H shift		
statistic	^{13}C	exptl (ppm)	calcd (ppm)	^{1}H	exptl (ppm)	calcd (ppm)
	1	129.7	126.8	2	7.1	6.5
	2	109.0	110.1	OMe	3.9	3.9
	3	148.9	145.9	4-OH	7.4	8.8
	4	144.5	143.6	6	6.9	7.0
	5	123.2	124.2	α	6.5	6.2
	6	126.2	124.5	*β*	6.3	6.2
	α	130.6	133.6	*γ*	4.2	4.4
	β	128.5	126.2			
	γ	63.5	65.2			
	OMe	56.5	53.7			
slope			0.99			1.06
y-intercept (ppm)			0.45			−0.26
r^2			0.995			0.849
MUE (ppm)			2.1			0.4
RMSE (ppm)			2.2			0.6
ME (ppm)			3.0			1.4

[a] The shifts are Boltzmann averaged from six conformers (MG1—MG6) of the 5-5 linkage (Figures 1 and 2).

half the value of those for the B3LYP/6-311+G(2d,p) (5.1, 5.6, and 9.0 ppm, respectively) and HF/6-311+G(2d,p), (5.3, 5.8, and 10.0 ppm, respectively) methods (Table 2 and Figure 3a,c,d). Furthermore, the multistandard results (Figure 3a) also show better agreement with experiment than the results obtained from the TMS-standard, mPW1PW91/6-31G(d) method (Figure 3b). Figure 3a clearly shows the better linear fit and lesser RMSE error bar values for the multistandard method, compared with the TMS-standard methods (Figure 3b−d). The strong linear correlation, small errors, and a faster calculation time due to a smaller basis set all indicate that the multistandard mPW1PW91/6-31G(d) method is more accurate and preferable for calculating ^{13}C NMR chemical shifts for MG than the TMS-based methods.

The linear correlation and error results for the ^{1}H calculations (Table 2 and Figure 4) indicate that only the multistandard mPW1PW91/6-31G(d) was able to quantitatively match with the data in acetone (Figure 4a). While the correlation coefficient (r^2) is only 0.901 (Table 1) for the multistandard ^{1}H calculation method, the r^2 values for the TMS-standard methods are all <0.8. Additionally, the MUE, RMSE, and ME (in ppm) for the multistandard method (0.3, 0.5, and 0.9 ppm, respectively) are one-half or less than those obtained from the TMS-standard methods. Figure 4a clearly illustrates the superiority of the multistandard method to the TMS-based methods (Figure 4b−d), based on linear fits and the RMSE error bars. The ^{1}H results indicate that the multistandard method is quantitatively superior to the TMS-standard methods based on a better linear fit and lower errors, with respect to the data. However, the results of the multistandard ^{1}H NMR calculations are less robust than those obtained for ^{13}C because the relative errors are much greater for the ^{1}H calculations relative to the chemical shift ranges, as compared to the errors for the ^{13}C NMR calculations.

Although the calculation of ^{1}H NMR shifts has proven statistically inferior to calculations for ^{13}C NMR shifts using the multistandard or the TMS-standard methods for MG (Table 2 and Figures 3 and 4), another result from the ^{1}H multistandard calculations is noteworthy. Using aliphatic H atoms from methanol as the standard for hydroxyl-H atoms resulted in a large underestimation of the hydroxyl-H shift, with respect to the experimental shift. For example, the experimental NMR shift reported for the 4OH atom in acetone is 7.6 ppm;[4] if one uses the aliphatic H-atoms of methanol with the Boltzmann-averaged, multistandard calculation for 4OH of MG, the result is a 4.1 ppm shift. Conversely, if one uses the shift for the hydroxyl-H of methanol as the standard, the calculated shift is 8.6 ppm, which overestimates, but more closely approximates, the experimental shift of 7.6 ppm (Table 2). The calculated H-shift in acetone using the TMS-standard method for MG was 5.8, 5.8, and 5.4 ppm for the B3LYP, HF, and mPW1PW91 methods, respectively, which also underestimate the 7.6 ppm experimental shift. Moreover, using the hydroxyl-H of phenol as the NMR standard resulted in a chemical shift of 5.4 ppm for the nucleus; therefore, using a reference compound similar to the compound of interest did not improve the agreement with the NMR data. Similar discrepancy with experiment occurs for the *γ*-OH ^{1}H of MG (Table 2); the multistandard method again calculates a chemical shift (4.4 ppm), which is closer to the experimental value (3.8 ppm) than those calculated by the TMS-standard B3LYP (1.7 ppm), HF (2.1 ppm), or mPW1PW91 (1.3 ppm) methods. The discrepancies for the hydroxyl-H shifts are clearly visible in Figure 4b−d. These results indicate that the hydroxyl-H of methanol may be a more appropriate multistandard calculation of hydroxyl-H NMR shifts than the shifts from the aliphatic H nuclei of methanol.

The results from the calculations using $CHCl_3$ or DMSO as the solvent for calculating ^{13}C NMR shifts agreed with the acetone solvated results; the calculations in the three solvents all indicate that the multistandard method is superior to the TMS-standard method for calculating ^{13}C NMR chemical shifts (Table 3). Note that data was only available for ^{1}H NMR shifts in acetone,[4] so no comparison was possible between $CHCl_3$ or DMSO solvated MG or the MG dimers.

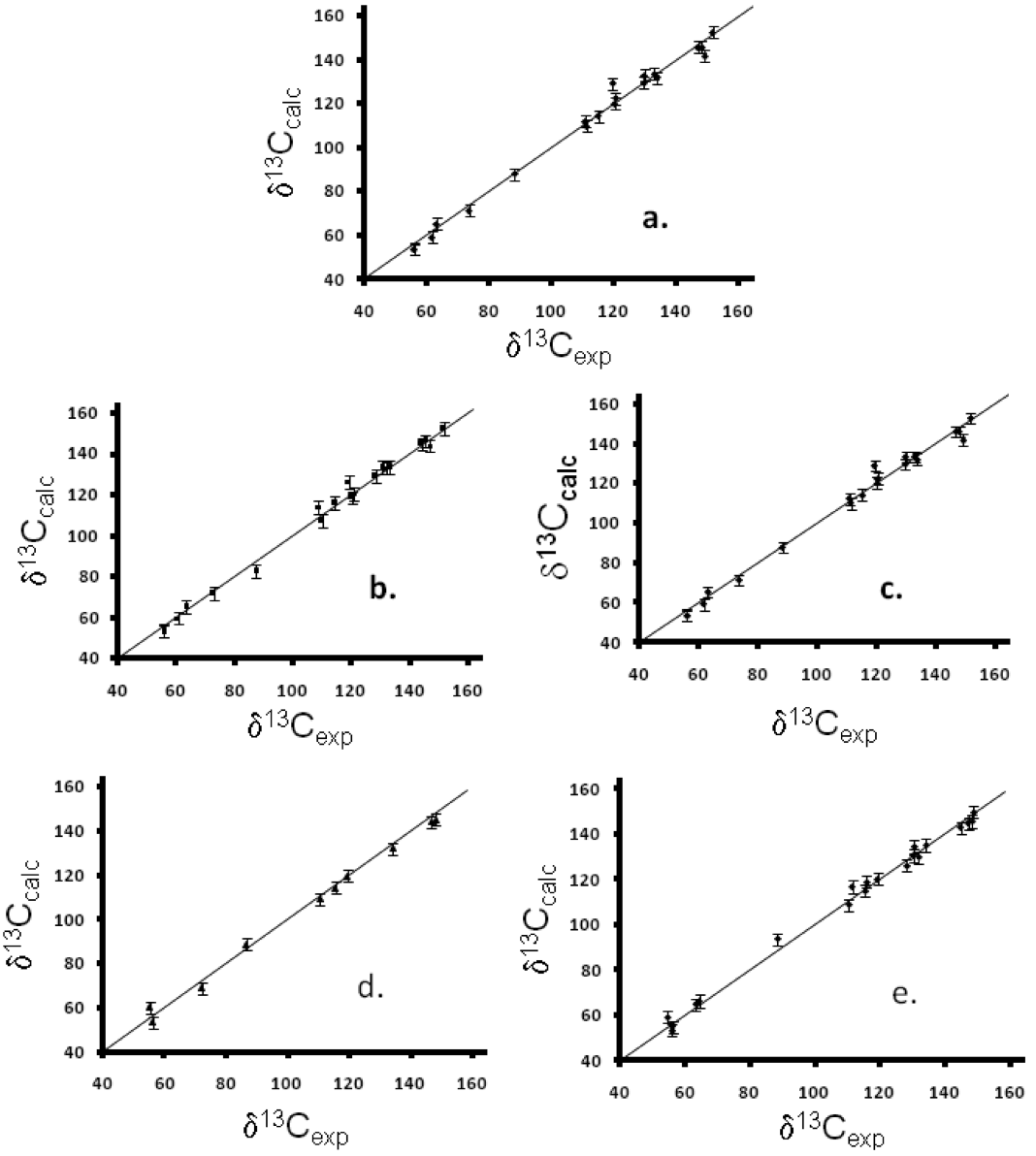

Figure 5. δ ^{13}C NMR data vs results for the (a) 5-5, (b) *threo* β-O-4, (c) *erythro* β-O-4, (d) β-5, and (e) β-β dimers of coniferyl alcohol (Figure 1). All NMR calculations were performed with the mPW1PW91/6-31G(d)//B3LYP/6-311++G(d,p) multistandard method. For all graphs, the solid line is the 1:1 line, where δ $^{13}C_{calc} = \delta$ $^{13}C_{exp}$. Results for the 5-5 dimer (a) are for the Boltzmann averaged NMR shifts for all six MG conformers (Figure 2); all other results are for Boltzmann averaged MG2 and MG5 conformers. All NMR shifts (δ ^{13}C) are in ppm. The RMSE error, shown by the error bars, is 2.2, 3.2, 2.7, 2.7, and 2.7 ppm for plots a−e, respectively.

Multistandard NMR Calculations Applied to Coniferyl Alcohol Dimers. The 5-5 dimer (Figure 1) of MG was used to determine if the MG2 and MG5 conformer forms were the most energetically prevalent, as the results from the MG monomer calculations indicate (Table 1). Table 4 shows the Boltzmann-weighted energies for the six forms of MG (Figure 2), which were used to construct the 5-5 dimer. An additional MG2/MG3 based hybrid dimer was included in the conformer set and was used for obtaining the Boltzmann averaged chemical shifts for this dimer. Data for the 5-5 dimer were only available in acetone, so results were not tabulated for the 5-5 dimer in the other solvents.[4] The results in Table 4 indicate that the MG2 and MG5 constitute 87% of the Boltzmann-distributed energy, based on the results for the seven conformers. Whereas the MG2/MG3 hybrid dimer contributed 12% of the conformational mixture, it was not used further; however, this result also reinforces the importance of using a large, but computationally feasible, set of conformers. The Boltzmann-weighted ^{13}C NMR shift statistics for the slope, y-intercept, r^2, MUE, RMSE, and ME using seven MG conformers were 0.99, 0.45, 0.995, 2.1, 2.2, and 3.0 ppm. These results were negligibly different when compared with those obtained by using the Boltzmann-weighted results from only the MG2 and MG5 conformers of 0.99, 0.63, 0.995, 2.2, 2.3, and 3.1 ppm. The results for the ^{1}H NMR shifts were also negligibly different for the 5-5 dimer when the results were compared for the combination of the MG2 and MG5 conformers with a complete set of seven conformers. Therefore, on the basis of these results and the energetic prevalence of MG2 and MG5 conformer in the monomer calculations (Table 1), all further dimer calculations will be based only on these two conformer structures.

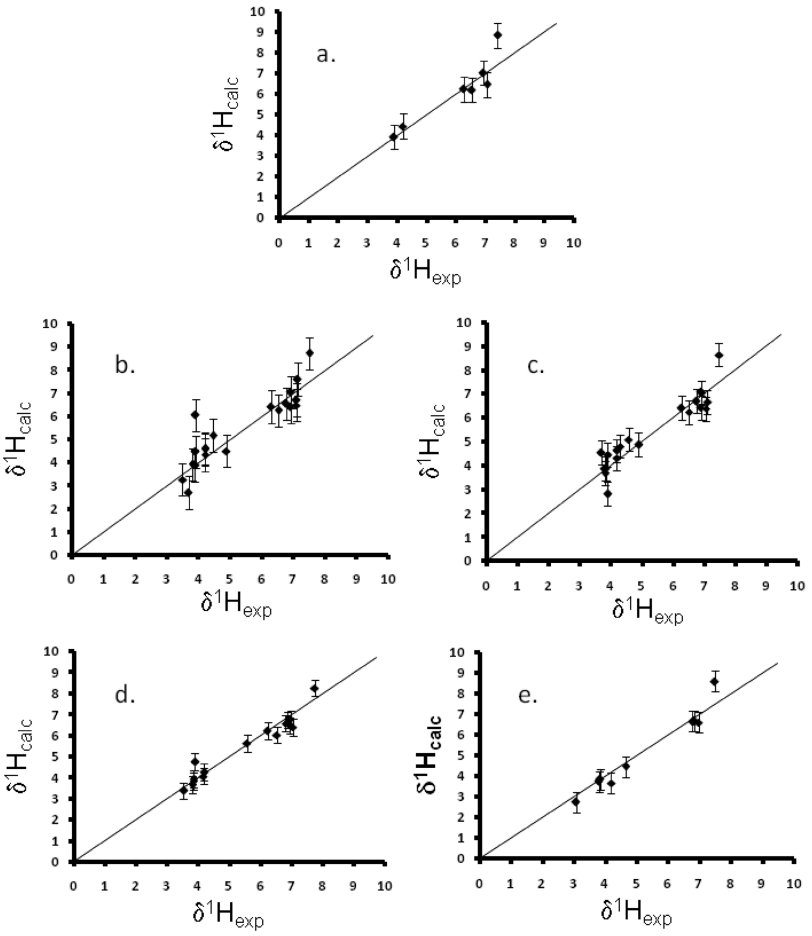

Figure 6. δ ^{1}H NMR data vs results for the (a) 5-5, (b) *threo* β-O-4, (c) *erythro* β-O-4, (d) β-5, and (e) β-β dimers of coniferyl alcohol (Figure 1). All NMR calculations performed with the mPW1PW91/6-31G(d)//B3LYP/6-311++G(d,p) multistandard method. For all graphs, the solid line is the 1:1 line, where δ $^1H_{calc}$ = δ $^1H_{exp}$. Results for the 5-5 dimer (a) are for the Boltzmann averaged NMR shifts for six MG conformers (Figure 2); all other results are for Boltzmann averaged MG2 and MG5 conformers. All NMR shifts (δ ^{1}H) are in ppm. The RMSE error, shown by the error bars, is 0.6, 0.7, 0.5, 0.4, and 0.5 ppm for plots a−e, respectively.

Table 5 and Figures 5a and 6a show the ^{13}C and ^{1}H NMR chemical shifts, regression statistics, and errors associated with the 5-5 dimer calculation in acetone. The ^{13}C NMR results exhibit an excellent correlation with the data and low associated errors (Table 5); Figure 5a shows the linear fit and RMSE errors for the 5-5 dimer along the 1:1 line. The results show an accurate fit with the data.

Table 5a and Figure 6a show the results for the ^{1}H NMR results for the 5-5 dimer. The r^2 value is 0.849, while the slope and intercept are approximately 0.96 and 0.22, respectively (Table 5). The MUE, RMSE, and ME are large, relative to the chemical shift range of ^{1}H (∼4−10 ppm). As with the MG monomer, the calculated shift (8.8 ppm) for the 4OH ^{1}H overestimates the experimental datum (7.4 ppm) for that shift.

Table 6 and Figures 5b,c and 6b,c contain the ^{1}H and ^{13}C NMR results for the β-O-4 linkage of MG. Although there are four possible stereoisomers for this linkage, only two combinations of the four forms are observable experimentally, the *threo* (RR and SS) and *erythro* (RS and SR) stereoisomers. For these calculations, the β-O-4 structures are based on either the MG2 or MG5 form of MG, on the basis of the argument from the MG and 5-5 results (Table 1 and Table 4). The Boltzmann weighting factors (Table 4) suggest that, for the *threo* form of the β-O-4 linkage, the SS stereoisomer is energetically favorable to the RR stereoisomer, and for the *erythro* form, the SR stereoisomer is energetically favorable to the RS stereoisomer. Moreover, the results predict that the MG5 based SS and SR stereoisomers are thermodynamically more stable than the MG2 based SS and SR stereoisomers. While these results are interesting, caution must be applied to these interpretations because of the following: (1) The SS and RR, and the RS and SR, stereoisomers are enantiomeric pairs; therefore, these enantiomer pairs are not differentiable with experimental NMR spectroscopy. (2) The calculations for the β-O-4 dimer are limited to a small sampling of possible conformers; future work, using multiple β-O-4 conformers is warranted by these results.

Additionally, the ΔG°_{solv} differences between the RR and SS enantiomers is <15 kJ/mol and the difference between the RS and SR enantiomers is <10 kJ/mol; these energy differences are of similar magnitude to a H-bond, and are therefore not significantly different. If these trends are true experimentally, these small energy differences, coupled with racemization, further prevent the differentiation of these enantiomers.

Overall, the calculated ^{13}C NMR shifts for *threo* and *erythro* forms of the β-O-4 linkage agree well with the data (Table 6 and Figure 5b,c), but there is a discrepancy between the calculated and

Table 6. Boltzmann-Averaged ^{13}C and ^{1}H NMR Shifts in Acetone for the β-O-4 Coniferyl Alcohol Linkage Using the Multistandard, mPW1PW91/6-31G(d)//B3LYP/6-311++G(d,p) Method[a]

		threo β-O-4 ^{13}C shift		*erythro* β-O-4 ^{13}C shift			*threo* β-O-4 ^{1}H shift		*erythro* β-O-4 ^{1}H shift	
statistic	^{13}C	exptl (ppm)	calcd (ppm)	exptl (ppm)	calcdd (ppm)	^{1}H	exptl (ppm)	calcd (ppm)	exptl (ppm)	calcd (ppm)
	A1	133.8	132.1	133.1	133.2	A2	7.1	6.7	7.1	6.7
	A2	111.4	109.8	110.1	107.1	A5	6.8	6.5	6.8	6.7
	A3	148.0	145.9	145.3	146.0	A6	6.9	6.4	6.9	6.4
	A4	146.8	145.8	144.0	144.6	Aα	4.9	4.5	4.9	4.9
	A5	115.2	114.2	114.4	115.8	Aβ	4.2	4.6	4.3	4.8
	A6	120.5	122.4	120.8	120.5	Aγ1	3.5	3.3	3.7	4.6
	Aα	73.8	71.1	73.0	71.7	Aγ2	3.7	2.7	3.8	3.7
	Aβ	88.4	88.0	87.3	82.5	AOMe	3.8	3.9	3.8	3.9
	Aγ	61.9	59.1	60.9	59.8	Aγ-OH	3.9	6.0	3.9	2.8
	AOMe	56.2	53.7	56.0	53.7	Aα-OH	4.5	5.2	4.6	5.1
	B1	133.0	133.5	131.9	132.9	A4-OH	7.5	8.7	7.5	8.6
	B2	110.9	112.0	108.8	113.9	B2	7.1	6.5	7.1	6.4
	B3	151.7	152.6	151.6	152.1	B5	7.1	7.6	6.9	7.0
	B4	149.2	141.8	146.8	143.8	B6	6.9	7.0	6.9	7.1
	B5	119.6	129.0	119.1	126.3	Bα	6.5	6.2	6.5	6.2
	B6	120.3	120.1	120.1	118.5	Bβ	6.3	6.4	6.3	6.4
	Bα	129.9	133.1	130.6	133.3	Bγ1	4.2	4.3	4.2	4.3
	Bβ	129.6	129.4	128.2	128.8	Bγ2	4.2	4.6	4.2	4.6
	Bγ	63.3	65.2	63.6	65.1	BOMe	3.9	3.9	3.8	3.9
	BOMe	56.3	53.5	56.0	53.2	Bγ-OH	3.9	4.5	3.9	4.5
slope			1.01		1.03			0.93		0.95
y-intercept (ppm)			−1.48		−2.77			0.50		0.37
r^2			0.990		0.993			0.806		0.875
MUE (ppm)			2.3		2.1			0.5		0.4
RMSE (ppm)			3.2		2.7			0.7		0.5
ME (ppm)			9.5		7.1			2.1		1.2

[a] The *threo* stereoisomers shifts are averaged from two R,R (MG2 or MG5 based) and two S,S (MG2 or MG5 based) stereoisomers, while the *erythro* stereoisomer shifts are Boltzmann-averaged from two R,S (MG2 or MG5 based) and two S,R (MG2 or MG5 based) stereoisomers of the β-O-4 linkage (Figures 1 and 2).

experimental shifts for C5 on the B ring (Figure 1) of both forms. The maximum error for both the *threo* (9.5 ppm) and the *erythro* (7.1 ppm) forms occurs at the B5-carbon on each model. This result also suggests that a more thorough conformational analysis of the β-O-4 dimer is warranted. Otherwise, the results show an excellent correlation with the data, with low MUE and RMSE errors and good linear correlation (Table 6 and Figure 5b,c).

The ^{1}H results for the β-O-4 linkages are less well correlated with the data; r^2 values for the *threo* and *erythro* enantiomer pairs are 0.806 and 0.875, respectively. Additionally, the MUE, RMSE, and ME are high, relative to those from the ^{13}C results. These models all contain four hydroxyl H atoms, one each at their respective Aα-OH, A4-OH, Aγ-OH, and Bγ-OH H (Table 6); as discussed previously, hydroxyl-H shifts are a source of error with these calculations. For the *threo* enantiomers, the Aγ-OH shift is the source of the ME or 2.1 ppm, while the ME for the *erythro* enantiomers is less, at 1.2 ppm.

Table 7 and Figure 5d show the ^{13}C NMR results for the β-5 linkage of MG (Figure 1), which were constructed with the MG2 and MG5 conformers, and the NMR results were Boltzmann averaged with the weighting factors (Table 4). These results show a strong linear correlation and relatively low errors, relative to the data. Table 7 and Figure 6d provide the results for the ^{1}H NMR shifts compared to the data; here the results show good correlation and relatively small errors, although the agreement with the ^{1}H data is not as strong as the accord with the ^{13}C data.

The Boltzmann-averaged ^{13}C NMR results for the β-β linkage (Table 8 and Figure 5e) demonstrate good agreement with the data, based on linear fit and error statistics. While the ^{1}H results are not as well fit to their respective data as the ^{13}C data for the β-β linkage, the linear fit is acceptable and the error statistics are satisfactory (Table 8 and Figure 6e).

^{13}C NMR results for the β-O-4, β-5, and β-β linkages in $CHCl_3$ and DMSO (Table 9) are comparable to those in acetone (Table 6−8), but the MEs for the β-O-4 linkage are slightly higher in DMSO. There was no data available for the 5-5 linkage in chloroform or DMSO in the source used.[4] For example, the ME for the *threo* β-0−4 linkage in acetone is 9.5 ppm (Table 6), while the ME for that model in DMSO is 13.5 ppm (Table 9). The ME for the β-O-4 calculations in all solvents consistently occurred at the B5 carbon, further emphasizing the need for a more complete conformational analysis of the β-O-4 linkage to match the data better. No ^{1}H NMR data were available for $CHCl_3$ and DMSO solvated dimers, so these results are not reported.

Table 7. Boltzmann-Averaged ^{13}C and ^{1}H NMR Shifts in Acetone for the β-5 Coniferyl Alcohol Linkage Using the Multistandard, mPW1PW91/6-31G(d)//B3LYP/6-311++G(d,p) Method[a]

	^{13}C shift			^{1}H shift		
statistic	^{13}C	exptl (ppm)	calcd (ppm)	^{1}H	exptl (ppm)	calcd (ppm)
	A1	134.4	135.0	A2	7.0	6.4
	A2	110.5	108.5	A5	6.8	6.6
	A3	148.4	145.5	A6	6.9	6.8
	A4	147.3	144.5	Aα	5.6	5.6
	A5	115.7	115.0	Aβ	3.5	3.4
	A6	119.6	120.2	AOMe	3.8	3.7
	Aα	88.5	93.4	A4-OH	7.7	8.3
	Aβ	54.7	59.2	Aγ	3.9	3.9
	Aγ	64.6	66.2	Aγ-OH	3.9	4.8
	AOMe	56.3	53.3	B2	6.9	6.5
	B1	131.9	129.5	B6	7.0	6.8
	B2	111.7	116.6	Bα	6.5	6.0
	B3	145.1	142.7	Bβ	6.2	6.2
	B4	148.8	149.7	BOMe	3.9	3.8
	B5	130.4	130.4	Bγ	4.2	4.3
	B6	116.1	118.8	Bγ-OH	4.2	4.1
	Bα	130.5	134.4			
	Bβ	128.3	126.1			
	Bγ	63.4	64.7			
	BOMe	56.4	55.0			
slope			0.98			0.93
y-intercept (ppm)			2.82			0.34
r^2			0.994			0.944
MUE (ppm)			2.3			0.3
RMSE (ppm)			2.7			0.4
ME (ppm)			4.9			0.9

[a] The shifts are Boltzmann-averaged from two conformers (MG2 or MG5 based) of the β-5 linkage (Figures 1 and 2).

Table 8. ^{13}C and ^{1}H NMR Shifts in Acetone for the β-β Coniferyl Alcohol Linkage Using the Multistandard, mPW1PW91/6-31G(d)//B3LYP/6-311++G(d,p) Method[a]

	^{13}C shift			^{1}H shift		
statistic	^{13}C	exptl (ppm)	calcd (ppm)	^{1}H	exptl (ppm)	calcd (ppm)
	1	134.2	132.1	2	7.0	6.6
	2	110.6	109.1	5	6.8	6.6
	3	148.3	145.1	6	6.8	6.7
	4	146.9	144.0	α	4.7	4.5
	5	115.5	114.3	β	3.1	2.7
	6	119.6	119.8	4-OH	7.5	8.6
	α	86.6	88.8	OMe	3.8	3.9
	β	55.2	60.3	γ1	3.8	3.7
	γ	72.2	69.0	γ2	4.2	3.7
	OMe	56.2	53.5			
slope			0.96			1.12
y-intercept (ppm)			2.78			−0.72
r^2			0.995			0.953
MUE (ppm)			2.4			0.3
RMSE (ppm)			2.7			0.5
ME (ppm)			5.1			1.1

[a] The shifts were Boltzmann-averaged from two conformers (MG2 or MG5 based) of the β-5 linkage (Figures 1 and 2).

Table 9. Boltzmann-Averaged ^{13}C NMR Chemical Shift Statistics for Coniferyl Alcohol Dimers in $CHCl_3$ or DMSO[a]

model	slope	*y*-intercept (ppm)	r^2	MUE (ppm)	RMSE (ppm)	ME (ppm)
threo β-O-4 ($CHCl_3$)	1.03	2.78	0.993	2.1	2.8	9.0
threo β-O-4 (DMSO)	1.01	0.57	0.986	2.7	4.0	13.5
erythro β-O-4 ($CHCl_3$)	1.03	−2.82	0.994	2.0	2.7	7.2
erythro β-O-4 (DMSO)	1.01	−0.40	0.990	2.3	3.4	10.6
β-β ($CHCl_3$)	0.96	4.05	0.994	2.2	2.8	6.7
β-β (DMSO)	0.97	2.94	0.994	2.0	2.6	6.4
β-5 ($CHCl_3$)	0.95	7.78	0.996	2.6	3.2	6.5
β-5 (DMSO)	0.98	4.10	0.992	2.7	3.3	6.7

[a] The statistics were based on Boltzmann-averaged results for the MG2 and MG5 conformers of coniferyl alcohol (Figure 1 and 2).

CONCLUSION

The multistandard approach in conjunction with Boltzmann averaging to calculate ^{13}C NMR shifts for coniferyl alcohol and four of its dimers was successful, on the basis of the comparison of the calculated results with the experimental data. The multistandard approach results more accurately matched MG experimental NMR data than the three TMS-standard methods evaluated. The multistandard method was not only more accurate, but also the calculations were approximately an order of magnitude faster using mPW1PW91/6-31G(d) GIAO NMR calculations than the standard B3LYP/6-311+G(2d,p) or HF/6-311+G(2d,p) NMR tensor calculations.

The importance of using Boltzmann-weighted NMR shifts, based on the $\Delta G°_{solv}$ of six energy-minimized structures, was paramount to the success of this work, because conformers that exhibit good NMR shift correlation with experiment may not be the most thermodynamically favorable. Use of the Boltzmann distribution for the 5-5 dimer also allowed the determination of the most favorable conformers (MG2 and MG5), which allowed a decrease in the number of conformers used for further dimer calculations. However, the relatively large maximum errors reported for the β-O-4 dimer calculations suggest that a larger number of conformers are needed to elucidate more fully the potential energy surface of this dimer, and to reproduce the experimental results for this important linkage.

The results indicate, due to smaller correlation coefficients and relatively large maximum error values, that ^{1}H NMR calculations using the multistandard method do not effectively model experimental NMR shifts for the models studied. However, the source of error for the ^{1}H NMR calculations is associated with the calculation of hydroxyl-H atoms and the choice of standard for modeling them; both TMS and aliphatic methanol H-atoms underestimate hydroxyl-H shifts by more than 3 ppm, whereas using the hydroxyl-H from methanol as a standard overestimates these shifts by approximately 1.5 ppm. Excluding hydroxyl-H atoms from the calculations does improve the correlation with data. Therefore, ^{1}H NMR calculations should be used only as a supplement to ^{13}C NMR calculations for coniferyl alcohol derivatives, until a suitable standard is found that provides good agreement with hydroxyl-H data.

The multistandard mPW1PW91/6-31G(d) method was effective for calculating Boltzmann-averaged ^{13}C NMR shifts using B3LYP/6-311++G(d,p) energy minimized coniferyl alcohol and its β-β, β-5, 5-5, and β-O-4 dimers coupled with single-point GIAO NMR tensor calculations using the mPW1PW91/6-31G(d) method. Further testing should take place with a larger lignin oligomer data set to verify these results. Moreover, on the basis of previously reported results,[25] and the results reported herein, the multistandard approach to NMR calculations might prove useful for a wide range of compounds, including plant cell wall components.

AUTHOR INFORMATION

Corresponding Author

*E-mail: jdk7@psu.edu.

ACKNOWLEDGMENT

Support for this project was provided by USDA National Needs Graduate Fellowship Competitive Grant 2007-38420-17782 from the National Institute of Food and Agriculture to H.D.W. This work was also supported in part through instrumentation funded by the National Science Foundation through Grant OCI-0821527. J.D.K. acknowledges support of the U.S. Department of Energy grant for the Energy Frontier Research Center in Lignocellulose Structure and Formation (CLSF) from the Office of Science, Office of Basic Energy Sciences, under Award DE-SC0001090. M.N.A.M. was supported by the USDA Grant "Improved Sustainable Cellulosic Materials Assembled Using Engineered Molecular Linkers." Computational support was provided by the Research Computing and Cyberinfrastucture group at the Pennsylvania State University. Discussions with Ming Tien, Brett Diehl, Nicole Brown, and other members of the Center for Nanocellulosics and CLSF are also acknowledged.

REFERENCES

(1) O'Sullivan, A. C. *Cellulose* **1997**, *4*, 173–207.

(2) Ralph, J.; Brunow, G.; Harris, P. J.; Dixon, R. A.; Schatz, P. F.; Boerjan, W. Lignification: Are Lignins Biosynthesized via simple Combinatorial Chemistry or via Proteinaceous Control and Template Replication? In *Recent Advances in Polyphenol Research*; Daayf, F., Lattanzio, V., Eds.; Blackwell: U.K., 2008; Vol. 1; pp 36−66.

(3) Boerjan, W.; Ralph, J.; Baucher, M. *Annu. Rev. Plant Biol.* **2003**, *54*, 519–546.

(4) Ralph, , S. A.; Ralph, , J.; Landucci, L. L. *NMR Database of Lignin and Cell Wall Model Compounds*; http://ars.usda.gov/Services/docs.htm?docid=10491, November 2004.

(5) Ralph, J.; Lundquist, K.; Brunow, G; Lu, F.; Kim, H.; Schatz, P. F.; Marita, J. M.; Hatfield, R. D.; Ralph, S. A.; Christensen, J. H.; Boerjan, W. *Phytochem. Rev.* **2004**, *3*, 29–60.

(6) Liang, H.; Frost, C.; Wei, X.; Brown, N. R.; Carlson, J. E.; Tien, M. *Clean: Soil, Air, Water* **2008**, *36* (8), 662–668.

(7) Sarkanen, S.; Chen, Y.-R. Towards a mechanism for macromolecular lignin replication. *Appita Annu. Conf. Proc.* **2005**, *59* (2), 407–414 .

(8) Davin, L. B.; Lewis, N. G. Dirigent phenoy radical coupling: advances and challenges. *Curr. Opin. Biotechnol.* **2005a**, *16*, 398–406.
(9) Davin, L. B.; Lewis, N. G. *Curr. Opin. Biotechnol.* **2005**, *16*, 407–415.
(10) Simon, J. P.; Eriksson, K. L. *Holzforschung* **1998**, *52* (3), 287–296.
(11) Simon, J. P.; Eriksson, K. L. *J. Mol. Struct.* **1996**, *384*, 1–7.
(12) Elder, T. J.; Ede, R. M. The 8th International Symposium on Wood and Pulping Chemistry. 1995, 115−122.
(13) Wei, K.; Luo, S.; Fu, Y.; Liu., L. *THEOCHEM* **2004**, *712*, 197–205.
(14) Durbeej, B.; Eriksson, L. A. Formation of β-O-4 lignin models—a theoretical study. *Holzforschung* **2003**, *57*, 466–478.
(15) Durbeej, B.; Kriksson, L. A. *Holzforschung* **2003b**, *57*, 150–164.
(16) Elder, T. J.; Worley, S. D. *Wood Sci. Technol.* **1984**, *18*, 307–315.
(17) Martínez, C.; Sedano, M.; Mendoza, J.; Herrera, R.; Rutiaga, J. G.; López, P. *J. Mol. Graphics Modell.* **2009**, *28*, 196–201.
(18) Martínez, C.; Rivera, J. L.; Herrera, R.; Rico, J. L.; Flores, N.; Rutiaga, J. G.; López, P. *J. Mol. Model.* **2008**, *14*, 77–81.
(19) Salazar-Valencia, P. J.; Pérez-Merchancano, T.; Bolívar-Marinéz, L. E. *Braz. J. Phys.* **2006**, *36* (3B), 840–843.
(20) Jalali-Heravi, M.; Masoum, S.; Shahbazikhah, P. *J. Magn. Reson.* **2004**, *171*, 176–185.
(21) Barsberg, S.; Matousek, P.; Towrie, M.; Jørgensen, H.; Felby, C. *Biophys. J.* **2006**, *90*, 2978–2986.
(22) Elder, T. *THEOCHEM* **2000**, *505*, 257–267.
(23) Foresman, J. B.; Frisch, A. Single Point Energy Calculations. In *Exploring Chemistry with Electronic Structure Methods*, 2nd ed.; Gaussian, Inc.: Pittsburgh, PA, 1996; pp 21−22.
(24) Cheeseman, J. R.; Trucks, G. W.; Keith, T. A.; Frisch, M. J. *J. Chem. Phys.* **1996**, *104* (14), 5497–5509.
(25) Sarotti, A. M.; Pellegrinet, S. C. *J. Org. Chem.* **2009**, *74*, 7254–7260.
(26) Barone, G.; Duca, D.; Silvestri, A.; Gomez-Paloma, L.; Riccio, R.; Bifulco, G. *Chem.—Eur. J.* **2002**, *8* (14), 3240–3245.
(27) Lawoko, M.; Henriksson, G.; Gellerstedt, G. *Holzforschung* **2006**, *60*, 156–161.
(28) Frisch, M. J.; Trucks, G. W.; Schlegel, H. B.; Scuseria, G. E.; Robb, M. A.; Cheeseman, J. R.; Montgomery, J. A., Jr.; Vreven, T.; Kudin, K. N.; Burant, J. C.; Millam, J. M.; Iyengar, S. S.; Tomasi, J.; Barone, V.; Mennucci, B.; Cossi, M.; Scalmani, G.; Rega, N.; Petersson, G. A.; Nakatsuji, H.; Hada, M.; Ehara, M.; Toyota, K.; Fukuda, R.; Hasegawa, J.; Ishida, M.; Nakajima, T.; Honda, Y.; Kitao, O.; Nakai, H.; Klene, M.; Li, X.; Knox, J. E.; Hratchian, H. P.; Cross, J. B.; Bakken, V.; Adamo, C.; Jaramillo, J.; Gomperts, R.; Stratmann, R. E.; Yazyev, O.; Austin, A. J.; Cammi, R.; Pomelli, C.; Ochterski, J. W.; Ayala, P. Y.; Morokuma, K.; Voth, G. A.; Salvador, P.; Dannenberg, J. J.; Zakrzewski, V. G.; Dapprich, S.; Daniels, A. D.; Strain, M. C.; Farkas, O.; Malick, D. K.; Rabuck, A. D.; Raghavachari, K.; Foresman, J. B.; Ortiz, J. V.; Cui, Q.; Baboul, A. G.; Clifford, S.; Cioslowski, J.; Stefanov, B. B.; Liu, G.; Liashenko, A.; Piskorz, P.; Komaromi, I.; Martin, R. L.; Fox, D. J.; Keith, T.; Al-Laham, M. A.; Peng, C. Y.; Nanayakkara, A.; Challacombe, M.; Gill, P. M. W.; Johnson, B.; Chen, W.; Wong, M. W.; Gonzalez, C.; Pople, J. A. *Gaussian 03, Revision E.01*; Gaussian, Inc., Wallingford CT, 2004.
(29) Foresman, J. B.; Frisch, A. Frequency calculations. In *Exploring Chemistry with Electronic Structure Methods*, 2nd ed.; Gaussian, Inc.: Pittsburgh, PA, 1996; pp 61−90.
(30) Wong, M. W. *Chem. Phys. Lett.* **1996**, *256*, 391–399.
(31) Kohn, W.; Sham, L. J. *Phys. Rev.* **1965**, *140* (4A), A1133–A1138.
(32) Hohenberg, P.; Kohn, W. *Phys. Rev.* **1964**, *136* (3B), B864–B871.
(33) Lee, C.; Yang, W.; Parr, R. G. *Phys. Rev. B* **1988**, *37*, 785.
(34) Becke, A. D. *J. Chem. Phys.* **1993**, *98*, 1372.
(35) Becke, A. D. *J. Chem. Phys.* **1993**, *98* (7), 5648.
(36) Krishnan, R.; Brinkley, J. S.; Seeger, R.; Pople, J. A. *J. Chem. Phys.* **1980**, *72* (1), 650–654.
(37) Clark, T.; Chandrasekhar, J.; Spitznagel, G. W.; von Ragué Schleyer, P. *J. Comput. Chem.* **1983**, *4* (3), 294–301.
(38) Bühl, M. NMR Chemical Shift Computation: Structural Applications. In *Encyclopedia of Computational Chemistry*; von Ragué Schleyer, P., Allinger, N. L., Clark, T., Gastiger, J., Kollman, P. A., Schaefer, H. F., III, Schreiner, P. R., Eds.; Wiley: New York, 1998, Vol. 3; pp 1835−1845.
(39) Fleischer, U.; van Wüllen, C.; Kutzelnigg, W. NMR Chemical Shift Computation: *Ab Initio*. In *Encyclopedia of Computational Chemistry*; von Ragué Schleyer, P., Allinger, N. L., Clark, T., Gastiger, J., Kollman, P. A., Schaefer, H. F., III, Schreiner, P. R., Eds.; Wiley: New York, 1998, Vol. 3; pp 1827−1835.
(40) Hu, C.; Chong, D. P. Density Functional Applications. In *Encyclopedia of Computational Chemistry*; von Ragué Schleyer, P., Allinger, N. L., Clark, T., Gastiger, J., Kollman, P. A., Schaefer, H. F., III, Schreiner, P. R., Eds.; Wiley: New York, 1998, Vol. 1; pp 664−678.
(41) Robien, W. NMR Data Correlation with Chemical Structure. In *Encyclopedia of Computational Chemistry*; von Ragué Schleyer, P., Allinger, N. L., Clark, T., Gastiger, J., Kollman, P. A., Schaefer, H. F., III, Schreiner, P. R., Eds.; Wiley: New York, 1998, Vol. 3; pp 1845−1857.
(42) Cancès, E.; Tomasi, J. *J. Phys. Chem.* **1997**, *107* (8), 3032–3041.
(43) Gogonea, V. Self-Consistent Reaction Field Methods: Cavities. In *Encyclopedia of Computational Chemistry*; von Ragué Schleyer, P., Allinger, N. L., Clark, T., Gastiger, J., Kollman, P. A., Schaefer, H. F., III, Schreiner, P. R., Eds.; Wiley: New York, 1998, Vol. 4; pp 2560−2574.
(44) Dumez, J.; Pickard, C. J. *J. Chem. Phys.* **2009**, *130*, 104701−1–104701−8.
(45) Johnston, J. C.; Iuliucci, R. J.; Facelli, J. C.; Fitzgerald, G.; Mueller, K. T. *J. Chem. Phys.* **2009**, *131*, 144503-1–144503-11.
(46) Szabo, A.; Ostlund, N. S. The Hartree Fock Approximation. In *Modern Quantum Chemistry*; Dover Publications. Mineola, NY, 1989; pp 108−230.
(47) Adamo, C.; Barone, V. *J. Chem. Phys.* **1998**, *108* (2), 664–675.
(48) National Institute of Advanced Industrial Science and Technology (AIST), http://riodb01.ibase.aist.go.jp/sdbs/cgi-bin/cre_index.cgi.
(49) Wiitala, K. W.; Cramer, C. J.; Hoye, T. R. *Magn. Reson. Chem.* **2007**, *45*, 819–829.